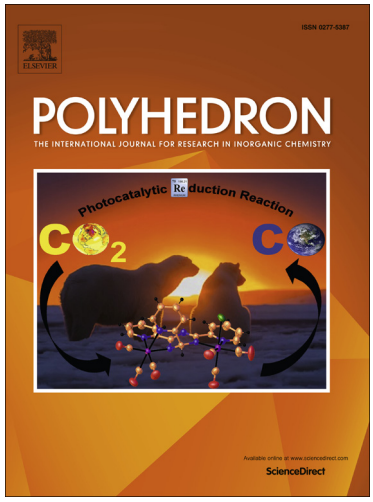

Naked-Eye Fluorescent Sensor for Cu (II) Based on Indole Conjugate BODIPY Dye

Sureyya O. Tümay, Elif Okutan, Ibrahim F. Sengul, Emrah Özcan, Hakan Kandemir, Tuğrul Doruk, Metin Çetin, Bünyemin Çoşut

PII: S0277-5387(16)30209-1
DOI: http://dx.doi.org/10.1016/j.poly.2016.05.056
Reference: POLY 12030

To appear in: *Polyhedron*

Received Date: 4 March 2016
Accepted Date: 29 May 2016

Please cite this article as: S.O. Tümay, E. Okutan, I.F. Sengul, E. Özcan, H. Kandemir, T. Doruk, M. Çetin, B. Çoşut, Naked-Eye Fluorescent Sensor for Cu (II) Based on Indole Conjugate BODIPY Dye, *Polyhedron* (2016), doi: http://dx.doi.org/10.1016/j.poly.2016.05.056

Naked-Eye Fluorescent Sensor for Cu (II) Based on Indole Conjugate BODIPY Dye

Sureyya O. Tümay[a] , Elif Okutan[a], Ibrahim F. Sengul[a], Emrah Özcan[a], Hakan Kandemir[b], Tuğrul Doruk[c], Metin Çetin[c], Bünyemin Çoşut[a*]

Contribution from:

[a] Department of Chemistry, Faculty of Science, Gebze Technical University, Gebze, Kocaeli, Turkey

[b] Department of Chemistry, Faculty of Art and Science, Namık Kemal University, Tekirdag, Turkey

[c] Department of Molecular Biology and Genetics, Faculty of Science, Gebze Technical University, Gebze, Kocaeli, Turkey

[*]Author for correspondence:

Dr. Bünyemin Çoşut, Department of Chemistry, Gebze Technical University, P.O.Box: 141, Gebze 41400, Kocaeli, Turkey

Tel: 00 90 262 6053015

Fax: 00 90 262 6053105

e-mail: bc@gtu.edu.tr

Abstract

A novel on/off fluorescent indole\ BODIPY- based Cu^{2+} chemosensor (**3**) was synthesized by Knoevenagel condensation of BODIPY derivative **1** with 2-methyl-indole-3-carbaldehyde **2.** The identity of compound **3** was confirmed by ^{1}H NMR, ^{13}C NMR, FT-IR, matrix-assisted laser desorption/ionization time-of-flight mass spectrometry and single crystal x-ray diffraction techniques. Fluorescent chemosensor (**3**) is found to be highly selective and sensitive for detection of Cu^{2+} with a color change from purple to yellow. The optical sensor features for the Cu^{2+} complex of **3** were investigated by UV−vis and fluorescence spectroscopy. The addition of Cu^{2+} caused quenching of fluorescence intensity and the detection limit was calculated to be 0.124 μM. Also, the stoichiometry ratio of **3**+$\mathbf{Cu^{2+}}$ was obtained 2:1 by Job's plot. Live cell image, flow cytometry and cytotoxic properties of compound **3** were examined.

Keywords: Borondipyrromethenes, Indole, Cu^{2+} ion sensor, Fluorescence, Chemosensor,

1. Introduction

The design and construction of fluorescent chemosensors with high selectivity and sensitivity through metal ions such as iron, aluminium and copper has been the subject of intense study because of their potential application in supramolecular chemistry, organic chemistry, drug delivery, biological chemistry and environmental research [1-3]. Also, they have a significant sensitivity and selectivity for detecting metal ions in both aqueous and non-aqueous media [4-7] many chemosensors have been developed specific for Ca^{2+}, Hg^{2+}, Cu^{2+}, Zn^{2+} or other transition metals [8-13]. The selective recognition and sensing of soft metal ions is quite important as these cations play an important role in various biological processes, including iron absorption, haemopoiesis, various enzyme-catalyzed and redox reactions [14]. Among these transition metals, copper is known as third abundant transition metal element in human body and generally found as Cu (II) in natural water [15]. It is one of the most essential trace elements of importance for both physical and mental health and serves as a key co-factor for a wide variety of enzymes in living organism [16-19]. Copper overload can lead to vomiting, lethargy, increased blood pressure and respiratory rates, acute haemolytic anaemia, liver damage, neurotoxicity and neurodegenerative disease [20-21]. Furthermore, it can disrupt natural ecosystems due to their adverse effects on microorganism [22]. Recently, some fully water soluble fluorescence probes have been reported here represents the first example of cell-elective imaging. [23-25]. Consequently, much attention has been drawn to the development of highly selective fluorescent chemosensor for Cu^{2+} to satisfy the biological and environmental applications [26]. The limit for copper in drinking water, as set by the US Environmental Protection Agency (EPA) is 1.3 ppm (20 µM). Also, the average concentration of blood copper in the normal group is 5.7-23.6 µM.

Among the fluorescent sensors, boradiazaindacene (BODIPY) is one of the most important highly fluorescent dyes and extensively studied due to its excellent photo physical properties

such as high fluorescence quantum yield, large extinction, high photo-stability, long absorption and fluorescence wavelengths [27]. These dyes are widely used as optical chemosensor, fluorescent bio-labelling reagents, light harvesting materials and photodynamic therapy reagents have been broadly investigated [28-31]. In particular, BODIPY-based metallic cation sensors have attracted great deal of attention [32]. BODIPY based fluorescent chemosensor derivatives for selective detection of metal ions such as Fe^{3+}, Al^{3+} and Cu^{2+} was recently reported [33-34].

Indole is an aromatic heterocycle that is widely distributed in nature [35]. There has been a significant recent interest in synthesizing indole and its derivatives because of the utility of these compounds as fluorescence probe and also displayed wide range of biological activity such as anti-fungal, anti-inflammatory and anti-tumor properties [38-40].

Herein, we reported the facile synthesis of a new fluorescence chemosensor based on indole-conjugate mono-styryl BODIPY **3** which was served as reliable, more sensitive, more selective and more soluble for Cu^{2+} sensor. Compound **3** and Cu^{2+} ion complex were detected by UV-visible absorption and fluorescence emission methods. Also, properties of compound **3** in live cells, flow cytometry and bacterial and mammalian cells were investigated.

2. Experimental

2.1. Materials

The deuterated solvent ($CDCl_3$) for NMR spectroscopy, silica gel, dichloromethane and metal chlorides were provided from Merck. Following chemicals were obtained from Sigma Aldrich; 2,4-dimethylpyrrole, trifluoroacetic acid, 2,3-Dichloro-5,6-dicyano-1,4-benzoquinone, trimethylamine, Boron trifluoride diethyl etherate, glacial acetic acid, piperidine, 2-methylindole, phosphorus(V)oxychloride, *N*,*N*-dimethylformamide, benzene and

1,8,9-Anthracenetriol for the MALDI matrix was obtained from Fluka. All other chemicals used for the synthesis were reagent grade unless otherwise specified.

2.2. Equipment

Electronic absorption spectra were recorded with a Shimadzu 2101 UV spectrophotometer in the UV-visible region. Fluorescence excitation and emission spectra were recorded on a Varian Eclipse spectrofluorometer using 1 cm pathlength cuvettes at room temperature. The fluorescence lifetimes were obtained using Horiba- Jobin-Yvon-SPEX Fluorolog 3-2iHR instrument with Fluoro Hub-B Single Photon Counting Controller at an excitation wavelength of 470 nm. Signal acquisition was performed using a TCSPC module. Mass spectra were acquired in linear modes with average of 50 shots on a Bruker Daltonics Microflex mass spectrometer (Bremen, Germany) equipped with a nitrogen UV-Laser operating at 337 nm. ^{1}H and ^{13}C NMR spectra were recorded in $CDCl_3$ solutions on a Varian 500 MHz spectrometer. Analytical thin layer chromatography (TLC) was performed on silica gel plates (Merck, Kieselgel 60 Å, 0.25 mm thickness) with F_{254} indicator. Column chromatography was performed on silica gel (Merck, Kieselgel 60 Å, 230-400 mesh). Suction column chromatography was performed on silica gel (Merck, Kieselgel 60 Å, 70-230 mesh).

2.3. X-ray data collection and structure refinement

Unit cell measurements and intensity data collection were performed on an Bruker APEX II QUAZAR three-circle diffractometer using monochromatized Mo *Kα* X-radiation (λ = 0.71073 Å). Indexing was performed using APEX2 [41]. Data integration and reduction were carried out with SAINT V8.34A [42]. Absorption correction was performed by multi-scan method implemented in SADABS V2014/5 [43]. The structures were solved and refined using the Bruker SHELXTL Software Package [44]. All non-hydrogen atoms were refined anisotropically using all reflections with $I > 2\sigma(I)$. The C-bound H atoms were positioned

geometrically and refined using a riding mode. The N-bound H atoms were located from the difference Fourier map and restrained to be 0.89 Å from N atom using DFIX and their position were constrained to refine on their parent N atoms with *U*iso(H)= 1.2*U*eq(N). Crystallographic data and refinement details of the data collection are given in **Table 1**. The final geometrical calculations and the molecular drawings were carried out by Platon (version 1.17) and Mercury CSD (version 3.5.1) program [45-46].

2.4. Live Cell Imaging and Flow Cytometry

Bacterial and mammalian cells were analysed by Nikon Eclipse 80i fluorescence microscopy utilizing TritC filter (Ex:540/25 nm and Em:605/55 nm) and mammalian cells were analysed by BD Accuri C6 flow cytometer. For bacterial imaging Bacillus thuringiensis (Bt) vegetative cells and for mammalian cell imaging HuH7 cells were stained by 0.1 µM of compound **3** for 15 minutes. Flow cytometry analysis of HuH7 performed after staining of cells with 0.1 and 5 µM of compound 3 for 15 min.

2.5. Cytotoxicity Assays

Bacterial toxicity of 0.1 µM of compound **3** was analysed against 4 different bacterial cells namely, Pseudomonas Aeruginosa, Staphylococcus Aureus, Bacillus Cereus, Escherichia Coli. Colony forming units calculated and compared to DMSO treated control bacterial cells after 24 hours incubation. The viability of HuH7 cells were examined by The CellTiter 96® Aqueous One Solution Cell Proliferation Assay (Promega, USA) in 96-well culture plate format. HUH7 cells were treated with DMSO control and various concentrations (0.1, 0.5, 1, 5, 100 µM) of compound **3**. Absorbance was recorded at 490 nm using Varioskan™ Flash Multimode Reader (Thermo Scientific, USA).

3. Synthesis

Compound **1** was prepared with a minor revision by the procedure described previously [47]. The synthesis method of compound **2** was as follows based on literature [48] (**Scheme 1**).

3.1. Synthesis of compound 3

A 100 mL round bottomed flask was charged with benzene (50 mL) and purged with argon for 15 min. To a solution of BODIPY **1** (100 mg, 0.3 mmol) and 2-methyl-indole-3-carbaldehyde **2** (48 mg, 0.3 mmol) in benzene was added piperidine (0.2 mL) and glacial acetic acid (0.2 mL). The solution was refluxed in a Dean-Stark apparatus for 6h. The resultant was concentrated by evaporation, and the mixture was then extracted several times with dichloromethane/water. The combined extracts were dried over Na_2SO_4, evaporated under reduced pressure and purified by silica gel column chromatography using dichloromethane-hexane (5:2) as eluent to afford the compound **3**, yield: 70 mg, 50%.

Spectral data of **3**: (Found: C 74.89, H 5.57, N 8.98 %, $C_{29}H_{26}BF_2N_3$ (465) requires C 74.85, H 5.63, N 9.03%). ^{1}H NMR (500 MHz, $CDCl_3$) δ 8.18 (s, 1H), 8.05 (d, J = 7.8 Hz, 1H), 7.71 (d, J = 16.2 Hz, 1H), 7.48 (d, J = 6.3 Hz, 3H), 7.45 (s, 1H), 7.33 (d, J = 6.9 Hz, 2H), 7.20 (t, J = 7.5 Hz, 1H), 6.64 (s, 1H), 5.97 (s, 1H), 2.62 (s, 3H), 2.56 (s, 3H), 1.44 (s, 3H), 1.38 (s, 3H).^{13}C NMR (126 MHz, $CDCl_3$) δ 130.39, 129.10, 128.86, 128.67, 128.64, 123.04, 123.03, 122.68, 122.63, 122.56, 122.52, 121.68, 121.64, 120.46, 120.44, 120.37, 110.72, 110.70, 110.16, 110.14, 110.13, 110.07, 48.00, 47.64, 29.88, 29.86, 14.87, 14.36, 12.87. IR (ATR) υ_{max} (cm^{-1}): 3378 (secondary NH), 2955 (aromatic CH), 2918 (aliphatic CH), 2852 (aliphatic CH), 1605 (aromatic C=C), 1539 (aromatic C=C), 1503 (B-F), 1455 (aliphatic CH), 1370, (aliphatic CH), 1291 (C-N), 1194, 1146. MS (MALDI-TOF) m/z (%): 465 $[M]^+$, 446 $[M-F]^+$.

4. Results and Discussion

4.1. Synthesis and Structural Characterization

The synthetic route adopted here to prepare BODIPY-indole **3** is outlined in **Scheme 1**. Compound **3** was simply prepared by Knoevenagel condensation of a BODIPY derivative **1** with 2-methyl-indole-3-carbaldehyde **2** in a Dean–Stark apparatus using standard conditions in a moderate yield. The targeted mono-styryl BODIPY-indole compound **3** were easily separated from the side products via silica gel column chromatography. The structure of **3** was confirmed by FT-IR, ^{1}H, ^{13}C NMR, MALDI- MS and elemental analyses and the results were consistent with the assigned formulations. The mass spectrum of compound **3** was obtained by MALDI-TOF MS using dithranol as a MALDI matrix, and the spectrum revealed the peak groups representing the molecular ions at 465 Da and molecular ion rupture flour at 446 Da (**Fig S1**). The ^{1}H NMR of compound **3** showed three sets of methyl protons of BODIPY and one for indole unit appeared ~ 1.4 ppm and ~ 2.6 ppm, respectively. The β- pyrrolic signals of the compound **3** were noted as sharp singlets at 5.97 and 6.64 ppm. For the mono-styryl **3**, one of the β- pyrrolic protons is shifted to 6.64 ppm as the other remains at ~ 6 ppm. Aromatic protons of BODIPY and indole units were located at ~7-8 ppm region. In addition, the observed 16 Hz proton-proton coupling constant at 7.71 ppm proved an E conformation of the double bonds as expected. The N-H proton appeared as a singlet at 8.18 ppm (**Fig S2**). The solid state structure of the molecule **3** was further confirmed by X-ray crystallography (**Fig. 1**). Unit **3** crystallizes in the triclinic space group *P*-1 in the asymmetric unit cell (**Table 1**).

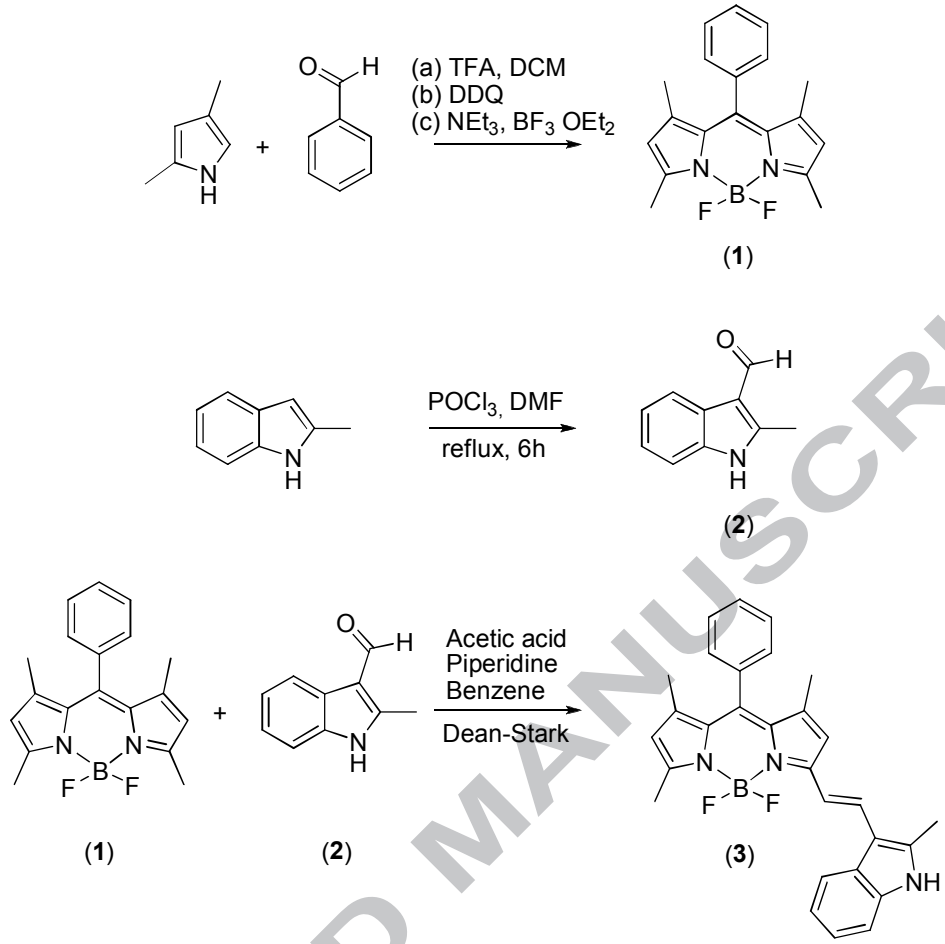

Scheme 1. Chemical structure and synthetic pathway of BODIPY-indole compound (**3**)

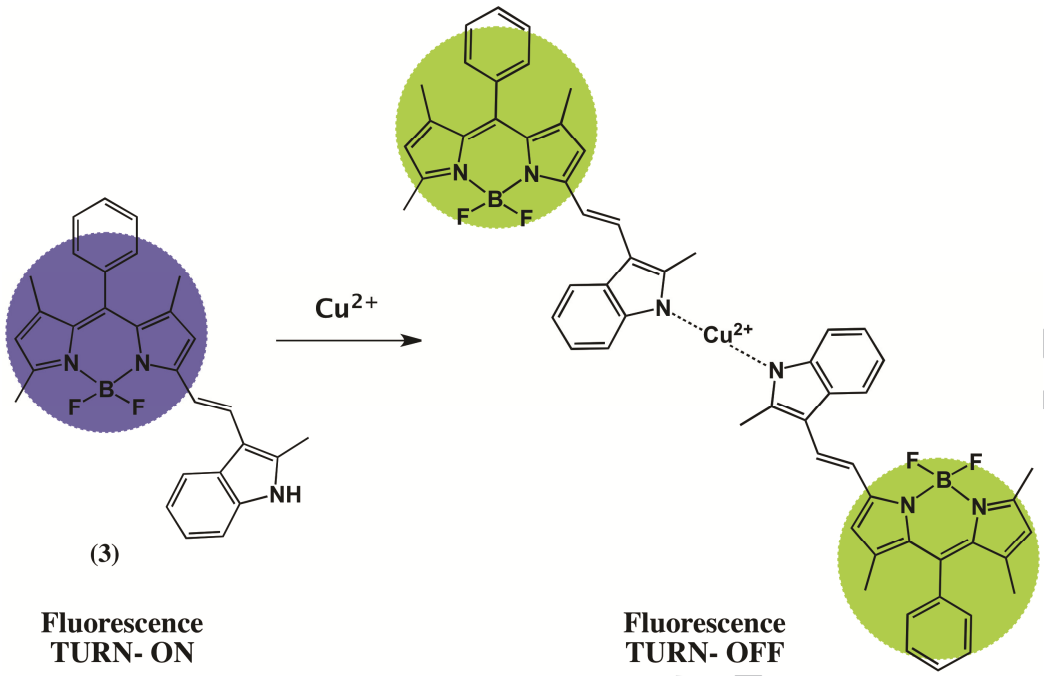

Scheme 2. Proposed binding mechanism of 3 with Cu^{2+}

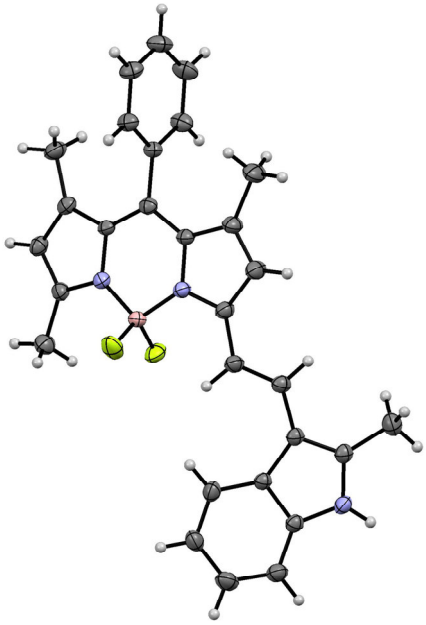

Fig. 1. The asymmetric unit of compound **3**. Displacement ellipsoids are drawn at the 30% probability level. H-atoms are shown as small spheres of arbitrary radii.

Table 1. Crystal data and refinement parameters for **3**.

Empirical Formula	$C_{29}H_{26}N_3BF_2$
Formula weight (g. mol^{-1})	465.34
Temperature (K)	293(2)
Wavelength (Å)	0.71073
Crystal system	Triclinic
Space group	*P* -1
a (Å)	9.9821(5)
b (Å)	11.4520(5)
c (Å)	12.5022(5)
α(°)	85.206(3)
β(°)	67.687(3)
γ(°)	67.139(3)
Crystal size (mm)	0.072 x 0.144 x 0.305
V (Å3)	1214.89(10)
Z	2
ρcalcd (g. cm^{-3})	1.272
μ (mm^{-1})	0.085
F(000)	488
θ range for data collection (°)	3.42 – 25.68
h/k/l	-12/12, -13/13, -15/15
Reflections collected	16342
Independent reflections	4603 [R(int) = 0.1028]
Absorption correction	Multi-scan
Data/restraints/parameters	4603 / 0 / 324
Goodness-of-fit on F^2	1.008
Final R indices [I > 2σ(I)]	R_1= 0.0587, wR_2= 0.1263
R indices (all data)	R_1= 0.1242, wR_2= 0.1528
Largest diff. peak and hole (e.Å^{-3})	0.281 and -0.270

4.2. Spectral Studies

The UV-Vis spectroscopic experiments of BODIPY-indole **3** were measured in acetonitrile with dilute solutions of $5x10^{-6}$ mol.dm^{-3} in the presence of 1 equivalent of various metal cations (Li^+, Na^+, K^+, Cs^+ ,Mg^{2+}, Ca^{2+}, Ba^{2+}, Hg^{2+} , Pb^{2+}, Mn^{2+}, Cd^{2+}, Ag^+, Ni^{2+}, Cu^{2+}, Zn^{2+}, Co^{2+}, Al^{3+}, Cr^{3+}, Fe^{3+}) as shown in **Fig. 2**. Compound **3** exhibited an absorption band at ~ 593 nm, characteristic for the mono-styryl BODIPY (**Fig S4a**) [49]. Upon addition of 1 equivalent of various metal ions, only Cu^{2+} induces the peak decreased which means **3** had higher binding affinity towards Cu^{2+} than other surveyed metal ions as a result of Pearson's Hard-Soft Acid-Base classification system in which Cu^{2+} acid and R_2NH bases are in the borderline [50].

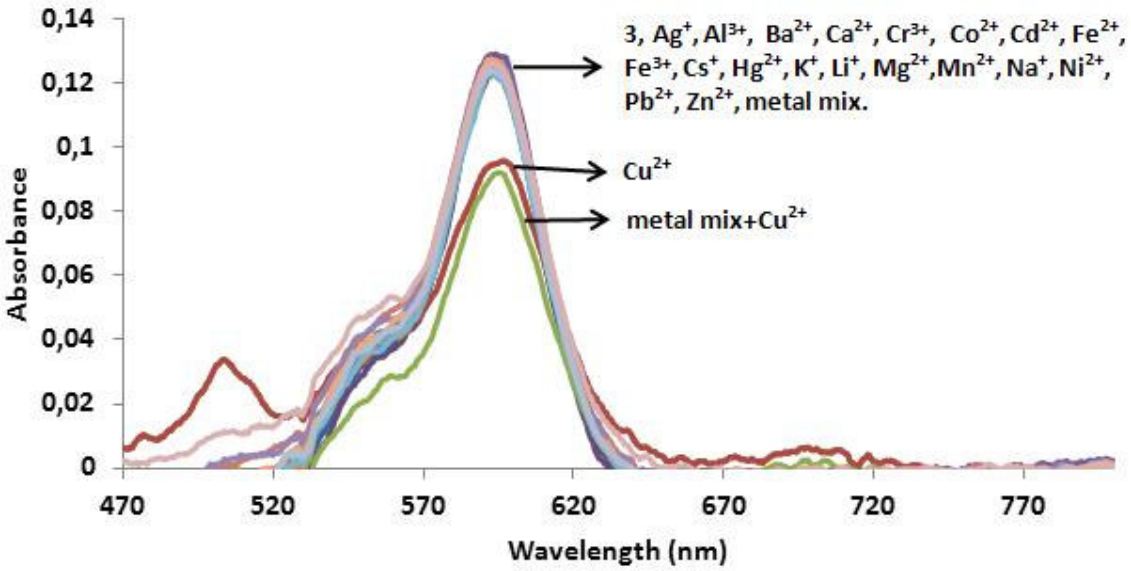

Fig. 2. UV–Vis absorption change profiles of compound **3** (5.0 μM) in CH_3CN with various metal ions (5.0 μM).

In order to obtain more information about binding mechanism of compound **3** towards Cu^{2+}, spectrometric titration experiments were performed in the presence of Cu^{2+}. While the sequential addition of Cu^{2+} ions from 0 to 2 equivalents to the solution of compound **3**

showed a gradual increase in absorbance at 506 nm, the other band at 593 nm showed a decrease in absorbance signal (**Fig. 3**). Consequently, **3** could serve as a sensitive fluorescent chemosensor for Cu^{2+} cations. The changes in the absorption curve of **3** could be assigned to a charge transfer transition occurring between the ligand and metal ion.

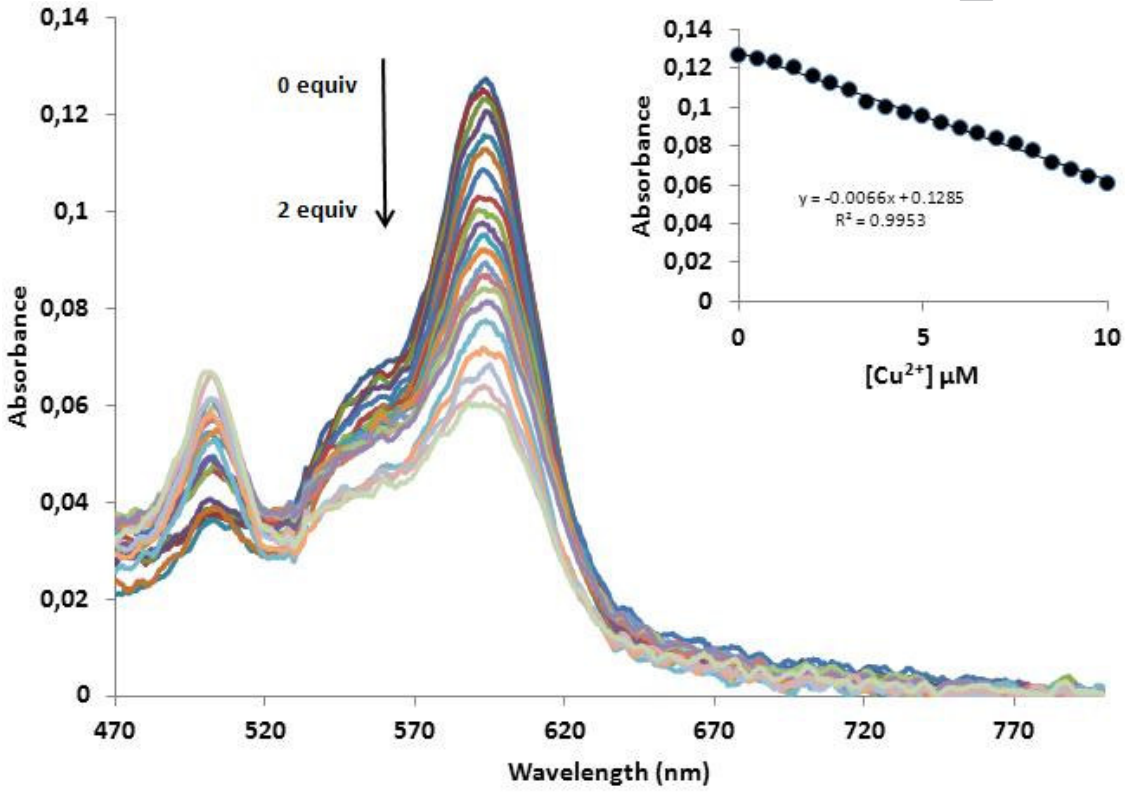

Fig. 3. UV–Vis absorption spectrum of **3** (5.0 µM) with gradual addition of Cu^{2+} in CH_3CN solution.

The fluorescence sensing of BODIPY-indole **3** was investigated on the aforementioned metal cations groups. The emission spectrum of **3** displayed a strong emission band at 635 nm when excited at 570 nm (**Fig S4b**). Except for Cu^{2+}, all tested metal ions caused minor changes in the emission band at 630 nm (characteristic for mono-styryl Bodipy emission) as shown in

Fig. 4. Upon addition of 1 equivalent of Cu^{2+} to the solution of **3**, remarkable decreasing of the fluorescent intensity of **3** is observed.

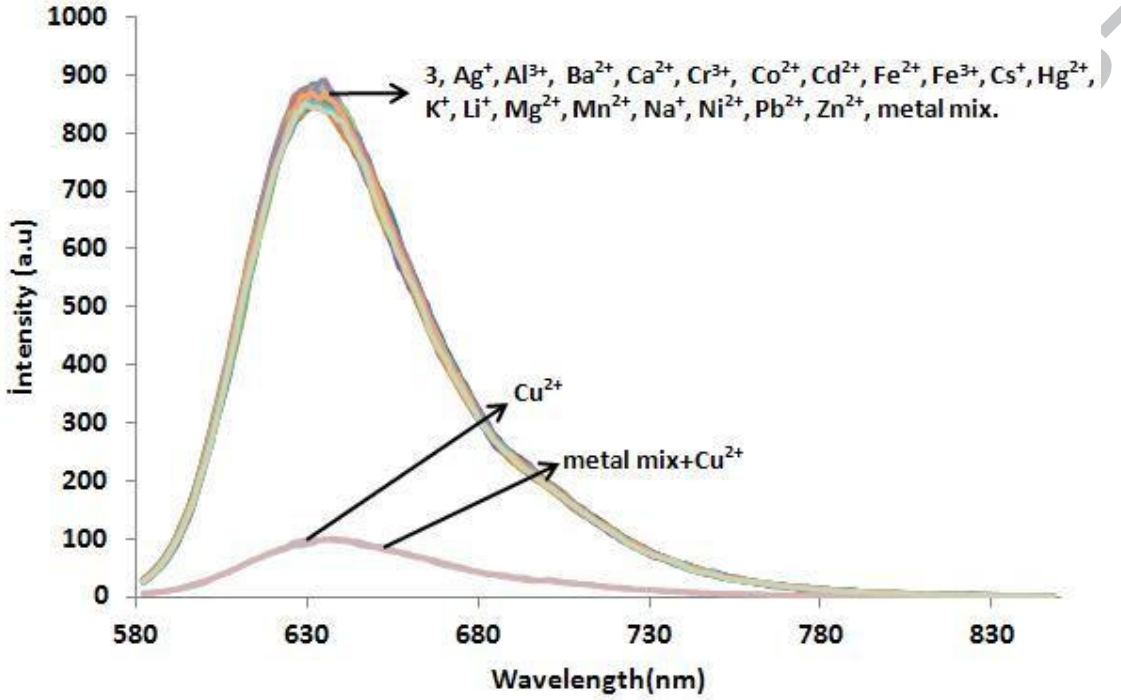

Fig. 4. Fluorescence responses of **3** (5.0 μM) in CH_3CN solution upon the addition of 1 equivalent of various metal ions (Excitation wavelength= 570 nm).

Furthermore, competition ion studies were also performed for **3** in the presence of Cu^{2+} at 5 μM that mixed with 5 μM of the tested metal cations such as Li^+, Na^+, K^+, Cs^+, Mg^{2+}, Ca^{2+}, Ba^{2+}, Hg^{2+}, Pb^{2+}, Mn^{2+}, Cd^{2+}, Ag^+, Ni^{2+}, Cu^{2+}, Zn^{2+}, Co^{2+}, Al^{3+}, Cr^{3+} and Fe^{3+} (**Fig. 5**). It was clearly found that the interference of other ions was insignificant during the detection of Cu^{2+}. Fluorescence titration experiments were also carried out in order to understand the binding mode of BODIPY-indole **3** with Cu^{2+} (**Fig. 6**). The fluorescence titration profile of compound **3** with Cu^{2+} in the range of 0 to 1.1 equivalents showed the Cu^{2+} detection limit. Time resolved fluorescence studies (using a 674 nm laser source and monitoring 630 nm as λ_{ems}) revealed a single exponential decay for **3** emissions and the lifetime was found to be 3.806

(±0.006) ns for molecule **3** and 0.261 (±0.009) ns for molecule **3**+Cu^{2+}. Changes in the lifetime from τ = 3.806 ns to τ = 0.261 ns clearly showed binding of Cu^{2+} to **3**. The detection limit of **3** for Cu^{2+} ion by fluorescence changes was calculated on the basis of 3σ /K [51-52] and found to be 0.124 μM pointing the high detection sensitivity (**Fig. 7**). These results suggested that **3** can be used for the selective detection of Cu^{2+} in acetonitrile solution.

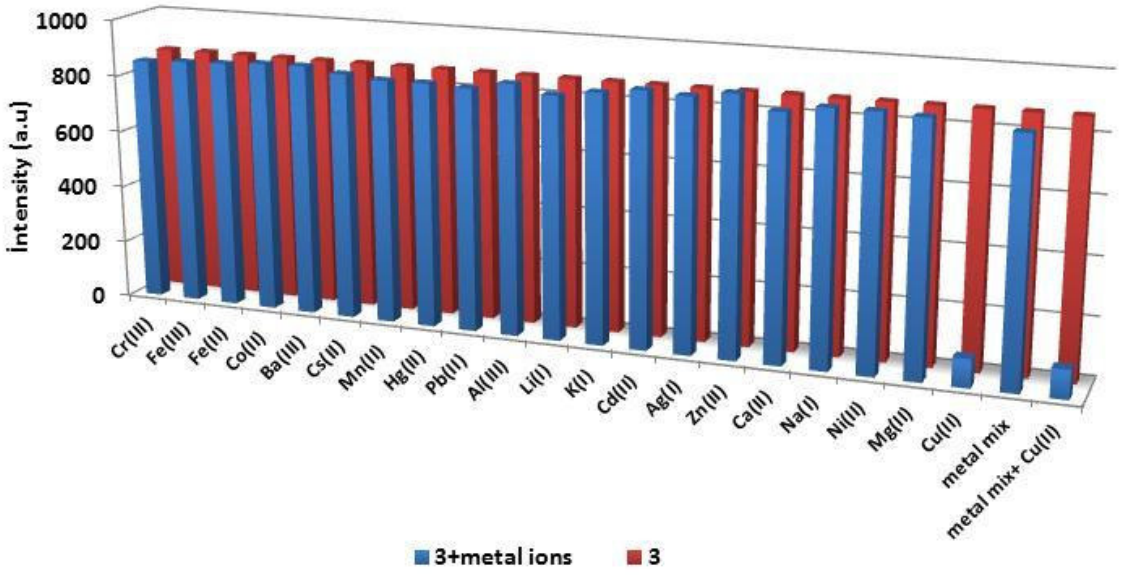

Fig. 5. Metal ions selectivity of molecule **3** (5.0 μM) in CH_3CN solution. The red bars represent the fluorescent intensity of only **3** and the blue bars represent the fluorescent intensity of **3** and various ions (Excitation wavelength= 570 nm).

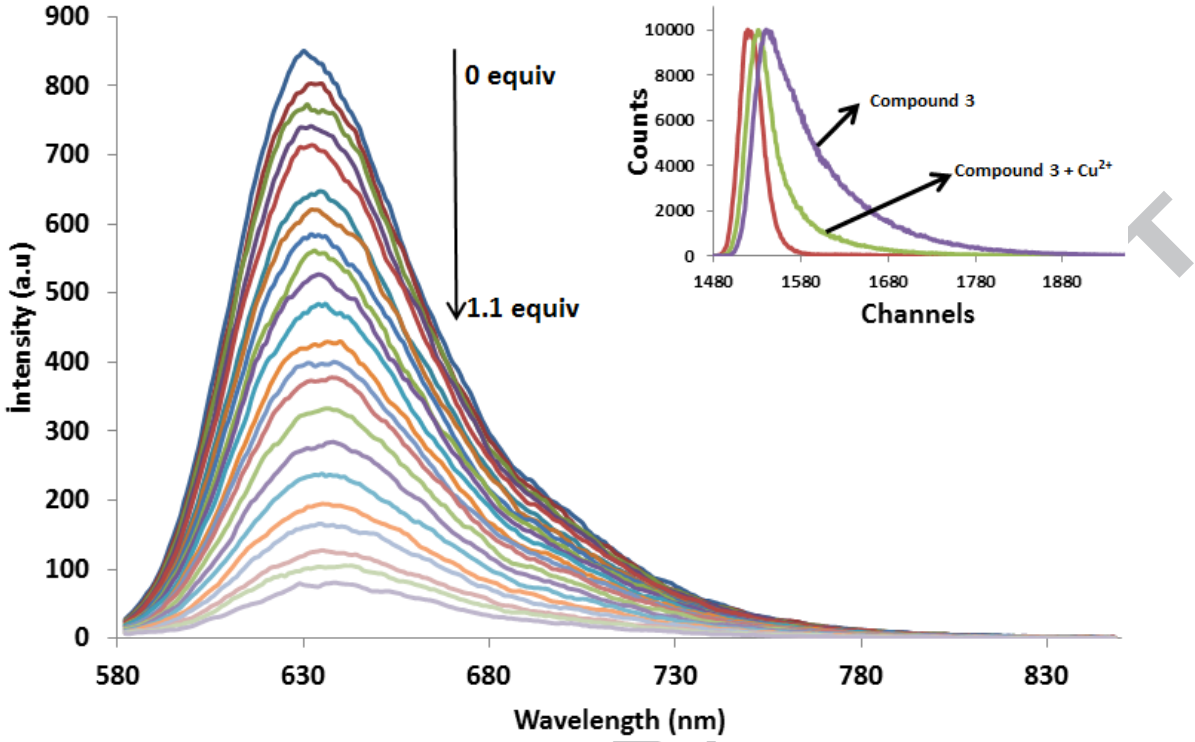

Fig. 6. Fluorescence titration of compound **3** (5.0 µM) with various concentration of Cu^{2+} in CH_3CN solution (Excitation wavelength= 570 nm). Inset: Fluorescence decay profile of compound **3** in the presence and absence of Cu^{2+} using laser excitation source of 674 nm.

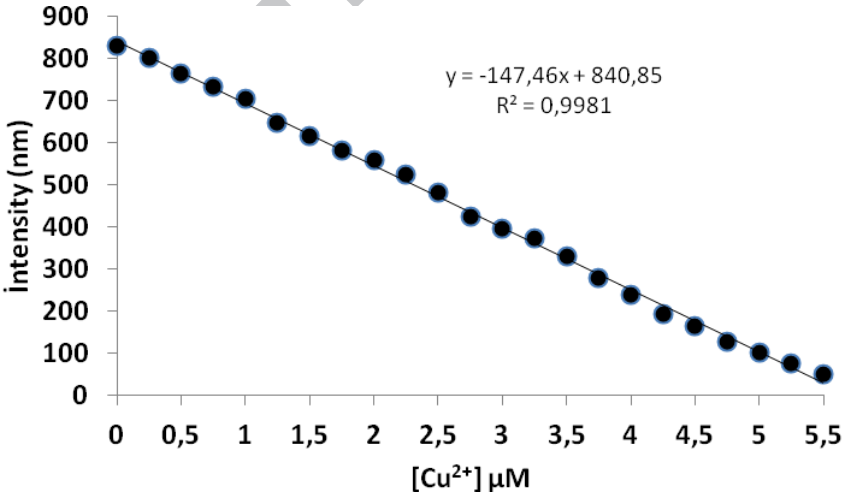

Fig. 7. Fluorescence intensity of **3** versus Cu^{2+} ions. [compound **3**] = 5 µM

Job's plot analyses were to use for investigating the stoichiometry between compound **3** and Cu^{2+} (**Fig. 8**). A Job's plot of **3** and Cu^{2+} indicated that the target complex exhibited a 2:1 ligand–metal ratio with a good linear relationship. This 2:1 stoichiometry was further confirmed by the MALDI-MS data with a peak of [**3+Cu**]$^{+}$ at m/z 993.6 (**Fig. S5**). The FT-IR spectra of the synthesized molecule **3** and target complex (molecule **3**-$\mathbf{Cu^{2+}}$) are also given in (**Fig. S6**). PET is often the cause of fluorescence quenching, when the PET process is followed by a nonluminescent process returning to the ground state [53]. The intense fluorescence of **3** is quenched by oxidative PET from the excited-state fluorophore to the indole moiety coordinated to Cu^{2+}. Cu^{2+} formed the most Stable 2:1 complex with **3** (**Scheme 2**). The structure of the **3** was confirmed by IR and the spectrum illustrated the N-H stretching band of indole secondary amine at ~3400 cm^{-1} and the aromatic C–H stretching bands were ~2900 cm^{-1}. After the complexation between compound **3** and Cu^{2+}; stretching vibration of secondary amine changed and shows two streches at 3440 cm^{-1} and 3340 cm^{-1} due to the complexation effect.

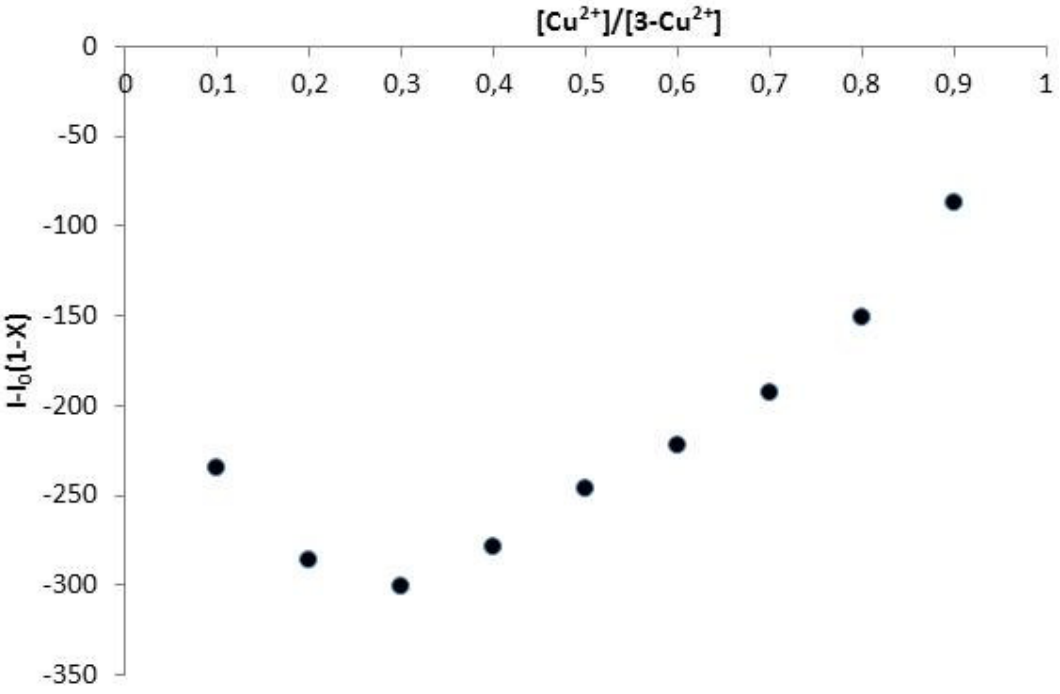

Fig. 8. The Job's plot for compound **3** and Cu $^{2+}$ (Excitation wavelength= 570 nm).

As shown in **Fig. 9**, the association constant K of the targeted complex was then calculated to be 1.53x10^{8} M^{-1} by the Benesi–Hildebrand equation.

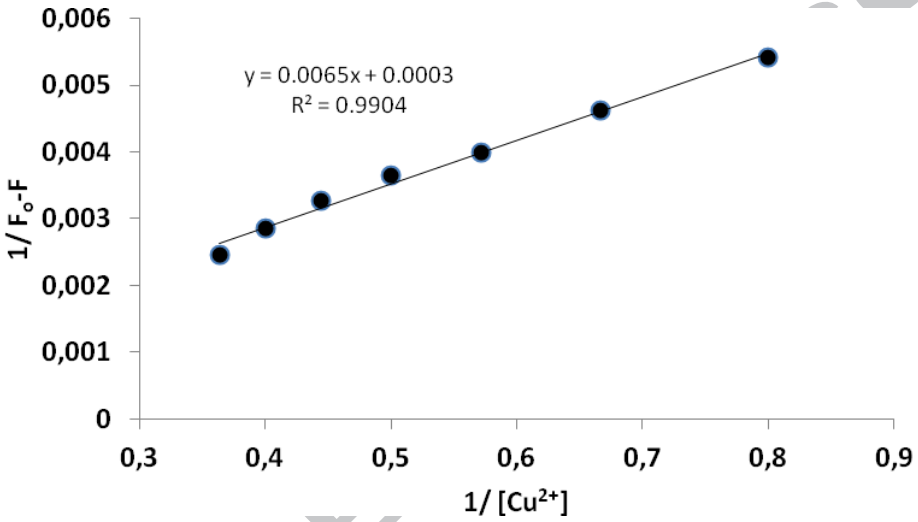

Fig. 9. Plot of 1/F-F$_0$ against **3**/[Cu $^{2+}$] for compound **3** in CH_3CN solution.

Moreover, **3** can detect Cu^{2+} in visual, and the visible color change can be easily observed by the addition of Cu^{2+}. In the presence of Cu^{2+}, a colour change of **3** was observed from purple to yellow followed by green under both sunlight and UV light (**Fig. 10**). Precision of the sensor is an important analytical parameter for sensor application. Therefore, ten measurements were performed for 5x10^{-6} M of Cu^{2+} under the same conditions. The relative standard deviation (RSD %) was calculated as 2.03 %. As a result, high reproducibility can provided for selected sensor.

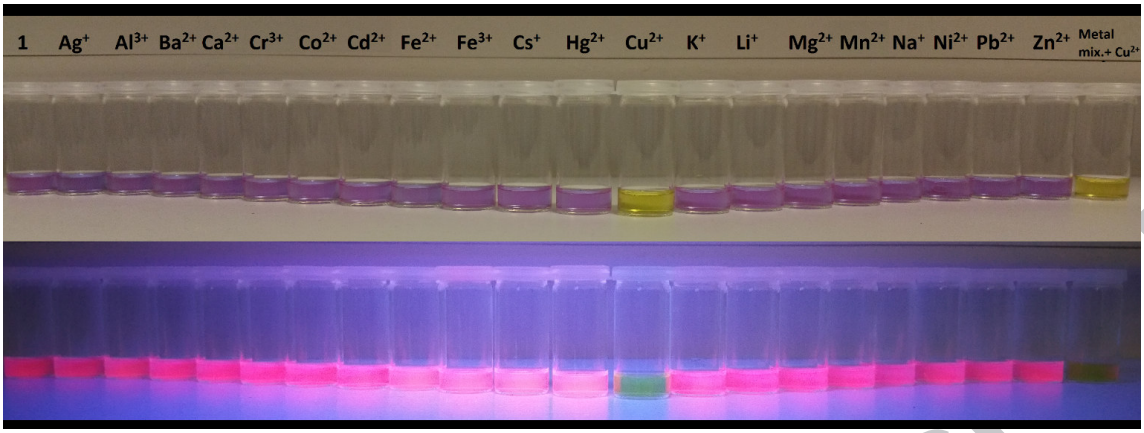

Fig. 10. Solution colour of molecule **3** exposed to various types of cations under sunlight (top) and UV light (bottom).

The photo stability is preferred for many fuorescent chemosensor dyes. The photo stability of **3** in the absence and presence of Cu^{2+} ion was investigated for 30 minutes in acetonitrile solution (**Fig. 11**). The fluorescence intensity of **3** and **3**-Cu^{2+} remain the same as initial value. Consequently, it was found that compound **3** and compound **3**-$\mathbf{Cu^{2+}}$ complexes have excellent photo stability.

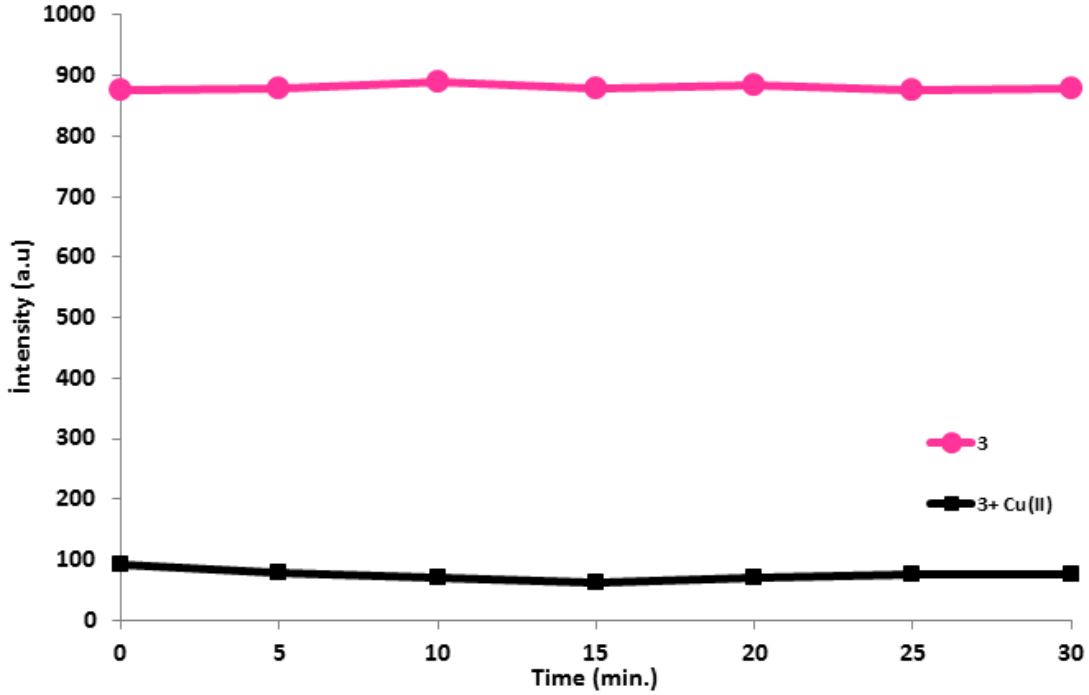

Fig. 11. The photo stability of **3** and **3**-Cu^{2+}. The change of fluorescence intensity with irradiation time for molecule **3** and compound **3**-Cu^{2+}.

4.3. Biological properties

BODIPY-indole **3** (0.1 µM) was used to explore the cellular staining of mammalian and bacterial cells. After 15 minutes incubation, both mammalian cells (**Fig. 12**) and bacterial cells (**Fig 13**) were stained efficiently. According to literature, it is quite important to stain cell without any damage for live cell imaging applications [54]. The fluorescence properties of **3** was analysed using flow cytometry and the results showed brighter fluorescence signals which were obtained from the stained cells in regard to increasing doses of **3** (0.1 and 5 µM) (**Fig. 14**). The toxicity of **3** was examined using bacterial and mammalian cell cultures. In this regard, bacterial cells were subjected to 100 µM of **3** and no toxic effect was observed (**Fig. 15a**). HuH7 cells were subjected to various concentrations (0.1, 0.5, 1, 5, 100 µM) of compound **3** and cytotoxicity was very low when compared to DMSO control cells (**Fig. 15b**). In the light of these findings, molecule **3** can serve as a biocompatible fluorescent agent

and stain bacterial/mammalian cells with low concentrations and it also showed promising potential for flow cytometry applications.

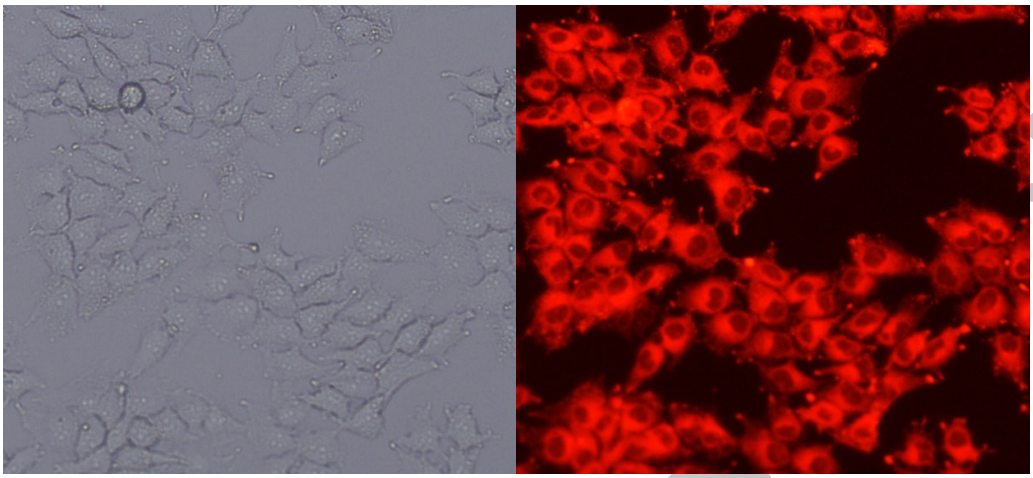

A **B**

Fig. 12. Fluorescent image of 3 in mammalian cells**.** HuH7 cells were treated with 0.1 μM of compound **3** and incubated for 15 minutes. **A.** Bright field image **B.** TritC filtered image.

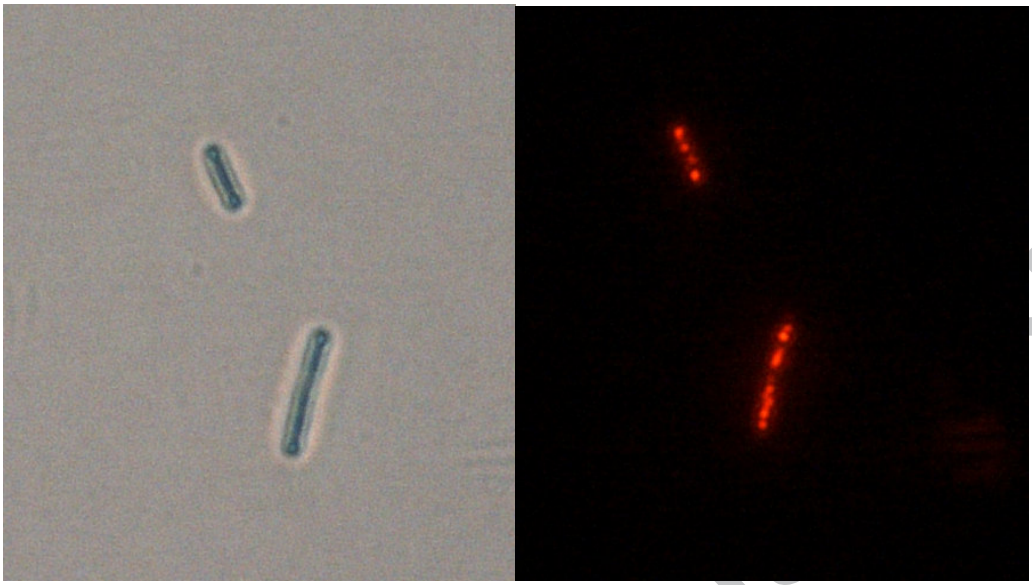

A **B**

Fig. 13. Fluorescent image of molecule **3** in bacterial cells**.** *Bacillus thuringiensis* cells were treated with 0.1 µM of **3** and incubated for 15 minutes. **A.** Bright field image. **B.** TritC filtered image.

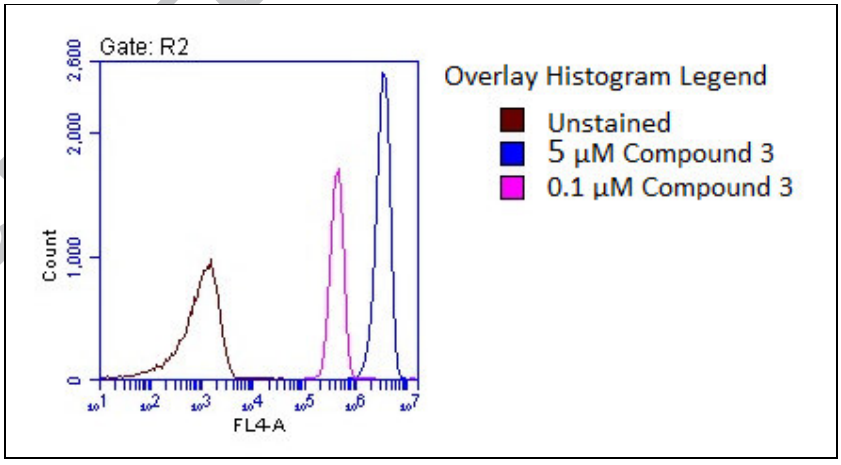

Fig. 14. Flow cytometry analysis of fluorescent **3** stained mammalian cells. HuH7 cells were stained with 0.1 µM and 5 µM of compound **3**. Overlay histogram of cells, unstained, stained

with both 0.1 μM of and 5 μM of **3**. Cell excited with red laser and data obtained from FL4: 675/25 nm filter.

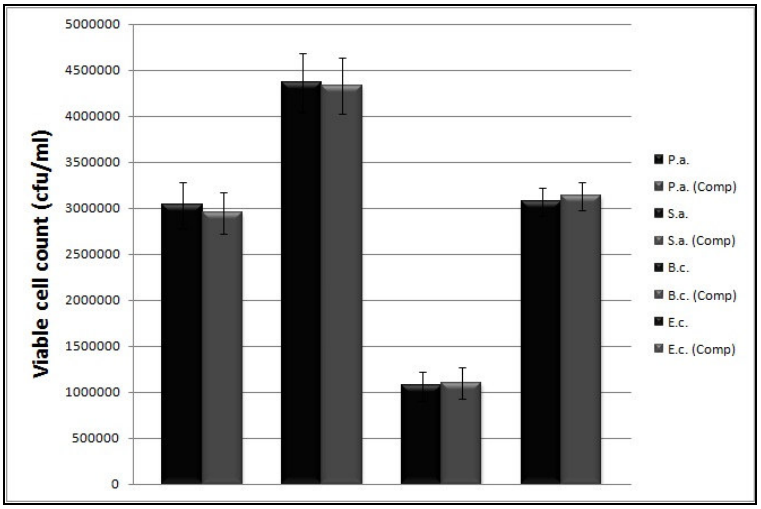

A

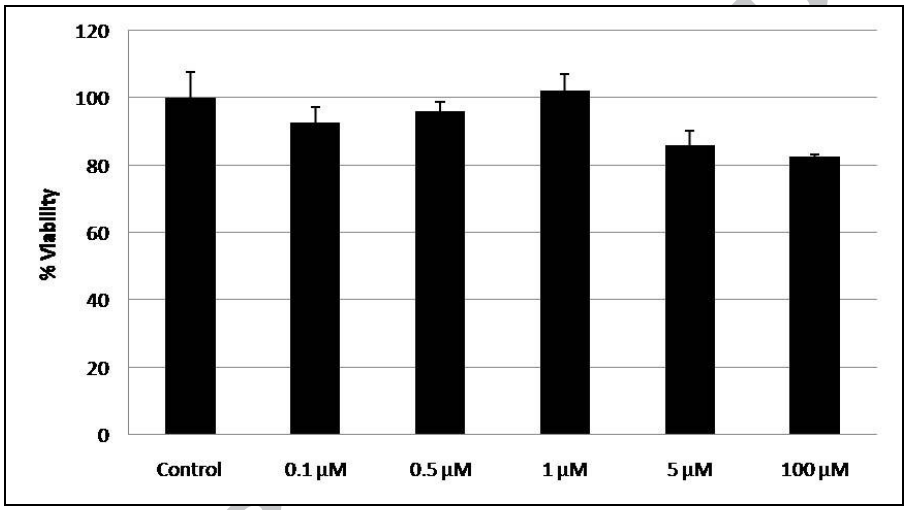

B

Fig. 15. Cytotoxic effects of **3** on bacterial and mammalian cells. **A.** Bacterial cells were treated with 100 µM of compound **3** and incubated for 24 hours. Viable cells count compared with DMSO treated control cells and calculated as cfu/ml. **B.** MTS assay results of HuH7 cells which were treated with 0.1, 0.5, 1, 5, 100 µM of compound **3** and incubated for 24 hours. Percentage of viable cells compared with DMSO treated control cells (set at 100%). Bars represent the corresponding standard deviations (n=3).

5. Conclusion

In conclusion, a novel indole mono-styryl BODIPY was successfully synthesised and characterized for the recognition of Cu^{2+}. It was found that **3** showed a remarkable selective and sensitive response towards Cu^{2+} by using UV-vis and fluorescence methods. According to Job's plot, binding stoichiometry was found by fluorescence method as 2:1 **3**+$\mathbf{Cu^{2+}}$. The detection limit of compound **3** was found to be 0.124 μM for Cu^{2+}. It was also revealed from this study **3** can passively diffuse through cell membrane and stain both bacterial and mammalian cells even in very low concentrations. BODIPY-indole **3** retains inside the cells in cytometry and can be further modified for other applications.

Acknowledgment

The CCDC number 1412690 contains the supplementary crystallographic data (CIF) for this article. These data can be obtained free of charge from the Director, CCDC, 12 Union Road, Cambridge CB2 1EZ, UK (Fax: +44-1223-336-033; e-mail: deposit@ccdc.cam. ac.uk or http://www.ccdc.cam.ac.uk).

References

[1] Gou C, Qin SH, Wu HQ, Wang Y, Luo J, Liu XY. A highly selective chemosensor for Cu^{2+} and Al^{3+} in two different ways based on Salicylaldehyde Schiff. Inorg Chem Commun 2011; 14:1622-25.

[2] Ghosh K, Saha I. Selective sensing of Zn(II) ion by a simple anthracene-based tripodal chemosensor. Tetrahedron Lett 2010; 51:4995-99.

[3] Azadbakht R, Keypour H. A new Schiff base system bearing two naphthalene groups as fluorescent chemodosimeter for Zn^{2+} ion and its logic gate behaviour. Spectrochim Acta A 2012; 85:293-97.

[4] Wang LN, Qin WW, Liu WS. A sensitive Schiff-base fluorescent indicator for the detection of Zn^{2+}. Inorg Chem Commun 2010; 13:1122-25.

[5] Bhalla V, Tejpal R, Kumar M. Terphenyl based fluorescent chemosensor for Cu^{2+} and F^{-} ions employing excited state intramolecular proton transfer. Tetrahedron Lett 2011; 67:1266-71.

[6] Udhayakumari D, Saravanamoorthy S, Ashok M, Velmathi S. Simple imine linked colorimetric and fluorescent receptor for sensing Zn^{2+} ions in aqueous medium based on inhibition of ESIPT mechanism. Tetrahedron Lett 2011; 52: 4631-35.

[7] Jiang JQ, Gou C, Luo J, Yi CL, Liu XY. A novel highly selective colorimetric sensor for Ni(II) ion using coumarin derivatives. Inorg Chem Commun 2012; 15:12-15.

[8] Delavaux NB, Maynadié J, Lavabre D, Fery FS. Ferrocenyl Compound as a Multiresponsive Calcium Chemosensor with Remarkable Fluorescence Properties in CH_3CN. Inorg Chem 2006; 45:5691-02.

[9] An JM, Yang ZY, Yan MH, Li TR. A novel off–on fluorescence chemosensor for Ca^{2+} based on Rhodamine–Coumarin Schiff base derivative. J Lumin 2013; 139:79-83.

[10] Singh TS, Paul PC, Pramanik HA. Fluorescent chemosensor based on sensitive Schiff base for selective detection of Zn^{2+}. Spectrochim Acta A 2014; 121:520-26.

[11] Cao W, Zheng XJ, Sun JP, Wong WT, Fang DC, Zhang JX, Jin LP. A Highly Selective Chemosensor for Al(III) and Zn(II) and Its Coordination with Metal Ions. Inorg Chem 2014; 53:3012-21.

[12] Mahato P, Saha S, Das A. Rare Example of TICT Based Optical Responses for the Specific Recognition of Cr^{3+} by a 2,2′:6′,2″-Terpyridine Derivative and Demonstration of Multiple Logic Operations. J Phys Chem C 2012; 116:17448-57.

[13] Dong M, Ma TH, Zhang AJ, Dong YM, Wang YW, Peng Y. A series of highly sensitive and selective fluorescent and colorimetric "off-on" chemosensors for Cu (II) based on rhodamine derivatives. Dyes Pigm 2010; 87:164-72.

[14] Malvankar PL, Shinde VM. Ion-pair extraction and determination of copper (II) and zinc(II) in environmental and pharmaceutical samples. Analyts 1991; 116: 1081-84.

[15] Li Q, Gou Y, Shao S. A BODIPY based fluorescent chemosensor for Cu(II) ions and homocysteine/cysteine. Sens Actuators B 2012; 171:872-77.

[16] Narayanaswamy N, Govindaraju T. Aldazine-based colorimetric sensors for Cu^{2+} and Fe^{3+}. Sens Actuators B 2012; 161:304-10.

[17] Maria JCM, Colin F, Barry HW, Graham HRC. A new use for an old molecule: **N**-phenyl-2-(2-hydroxynaphthalen-1-ylmethylene)hydrazinecarbothioamide as a ratiometric 'Off–On' fluorescent probe for iron. Tetrahedron Lett 2012; 53;670-73.

[18] Sahin AC, Tokgoz I. A novel solidified floating organic drop microextraction method for preconcentration and determination of copper ions by flow injection flame atomic absorption spectrometry. Anal Chim Acta 2010; 667:83-87.

[19] Linder MC, Hazegh-Azam M. Copper biochemistry and molecular biology. Am J Clin Nutr 1996; 63:797-811.

[20] Vulpe C, Levinson B, Whitney S, Packman S, Gitschier J. Isolation of a candidate gene for Menkes disease and evidence that it encodes a copper–transporting ATPase. Nat Genet 1993; 3:7-13.

[21] Bull PC, Thomas GR, Rommens JM, Forbes JR, Cox DW. The Wilson disease gene is a putative copper transporting P–type ATPase similar to the Menkes gene. Nat Genet 1993; 5:327-37.

[22] Kramer R. Fluorescent Chemosensors for Cu^{2+} Ions: Fast, Selective, and Highly Sensitive. Angew Chem Int Ed 1998; 37:772-73.

[23] Kai BL,Zang Y, Wang H, Li J, Chen GR, James TD, He XP and Tian H. Hepatoma-selective imaging of heavy metal ions using a 'clicked' galactosylrhodamine probe. Chem. Commun. 2014; 50:11735-37

[24] Shi DT, Zhou D, Zang Y, Li J, Chen GR, James TD, He XP and Tian H. Selective fluorogenic imaging of hepatocellular H2S by a galactosyl azidonaphthalimide probe Chem. Commun. 2015; 51: 3653-55

[25] Dong L, Zang Y, Zhou D, He XP, Chen GR, James TD, Li J, and Tian H. Glycosylation enhances the aqueous sensitivity and lowers the cytotoxicity of a naphthalimide zinc ion fluorescence probe Chem. Commun. 2015; 51: 11852-55

[26] Liu WY, Li HY, Lv HS, Zhao BX, Miao JY. A rhodamine chromene-based turn-on fluorescence probe for selectively imaging Cu^{2+} in living cell. Spectros Chim Acta A Mol Biomol Spectros 2012; 95:658-63.

[27] Ulrich G, Ziessel R, Harriman A. The Chemistry of Fluorescent Bodipy Dyes: Versatility Unsurpassed. Angew Chem Int Ed 2008; 47:1184-1201.

[28] Cheng T, Xu Y, Zhang S, Zhu W, Qian X, Duan L. A Highly Sensitive and Selective OFF-ON Fluorescent Sensor for Cadmium in Aqueous Solution and Living Cell. J Am Chem Soc 2008; 130:16160-61.

[29] Yee M, Fas SC, Stohlmeyer MM, Wandless TJ, Cimprich KA. Cell-permeable, Activity-based Probe for Protein and Lipid Kinases. J Biol Chem 2005; 280:29053–59.

[30] Goeb S, Ziessel R. Convenient Synthesis of Green Diisoindolodithienylpyrromethene–Dialkynyl Borane Dyes. Org Lett 2007; 9:737-40.

[31] Gorman A, Killoran J, O'Shera C, Kenna T, Gallagher WM, O'Shea DF. In Vitro Demonstration of the Heavy-Atom Effect for Photodynamic Therapy. J Am Chem Soc 2004; 126:10619-31.

[32] Zhang X, Xiao Y, Qian X. A Ratiometric Fluorescent Probe Based on FRET for Imaging Hg^{+2} Ions in Living Cells. Angew Chem Int Ed 2008; 47:8025-29.

[33] Kursunlu AN, Guler E, Ucan HI, Boyle RW. A novel Bodipy-Dipyrrin fluorescent probe: Synthesis and recognition behaviour towards Fe (II) and Zn (II). Dyes Pigm 2012; 94:496-502.

[34] Kursunlu AN. A fluorescent "turn on" chemosensor based on Bodipy–anthraquinone for Al(III) ions: synthesis and complexation/spectroscopic studies. RSC Adv 2015; 5:41025-32.

[35] Garg NK, Caspi DD, Stoltz BM. Development of an Enantiodivergent Strategy for the Total Synthesis of (+)- and (−)-Dragmacidin F from a Single Enantiomer of Quinic Acid. J Am Chem Soc 2005; 127:5970-78.

[36] Sakemi S, Sun HH. Nortopsentins A, B, and C. Cytotoxic and antifungal imidazolediylbis[indoles] from the sponge Spongosorites ruetzleri. J Org Chem 1991; 56: 4304-07.

[37] Lum GM, Aisenbrey GA, Dunn MJ, Berl T, Schrier RW, McDonald KM. In vivo effect of indomethacin to potentiate the renal medullary cyclic AMP response to vasopressin. J Clin Invest 1977; 59:8-13.

[38] Ahmad A, Sakr WA, Rahman KM. Anticancer properties of indole compounds: mechanism of apoptosis induction and role in chemotherapy. Current drug targets 2010; 11:652-66.

[39] Johnson IS, Cullinan GJ, Boder GB, Grindey CB, Laguzza BC. Structural modifications of the vinca alkaloids. Cancer Treat Rev 1987; 14:407-10.

[40] Eftink MR, Ghira CA. Indole fluorescence quenching studies on proteins and model systems: use of the inefficient quencher succinimide. Biochemistry 1984; 23:3891-99.

[41]Bruker (2014) APEX2, version 2014.11-0, Bruker AXS Inc., Madison, Wisconsin, USA

[42] Bruker (2013) SAINT, version V8.34A, Bruker AXS Inc., Madison, Wisconsin, USA.

[43] Bruker (2014) SADABS, version 2014/4, Bruker AXS Inc., Madison, Wisconsin, USA.

[44] Bruker (2010) SHELXTL, version 6.14, Bruker AXS Inc., Madison, Wisconsin, USA.

[45] Spek AL. Structure validation in chemical crystallography. Acta Cryst D, 2009; 65:148-55.

[46] Macrae CF, Edgington PR, McCabe P, Pidcock E, Shields GP, Taylor R, et al. Visualization and analysis of crystal structure. J Appl Cryst 2006; 39:453-57.

[47] Alamiry MAH, Benniston AC, Hagon J, Winstanley TPL, Lemmetyinen H, Tkachenko NV. The fluorine effect: photophysical properties of borondipyrromethene (bodipy) dyes appended at the meso position with fluorinated aryl groups. RSC Adv 2012; 2:4944-50.

[48] Sashidhara KV, Dodda RP, Sonkar R, Palnati GR, Bhatia G. Design and synthesis of novel indole-chalcone fibrates as lipid lowering agents. Eur J Med Chem 2014; 81:499-509.

[49] Bozdemir OA, Cakmak SE, Ekiz O, Dana A, Akkaya EU. Towards Unimolecular Luminescent Solar Concentrators: Bodipy-Based Dendritic Energy-Transfer Cascade with Panchromatic Absorption and Monochromatized Emission. Angew Chem Int Ed 2011; 50:10907-12.

[50] Pearson, Ralph G. "Hard and Soft Acids and Bases". J. Am. Chem. Soc. 1963, 85 (22): 3533–3539.

[51] C.A. Parker, W.T. Rees, Correction of fluorescence spectra and measurement of fluorescence quantum efficiency, Analyst. 1960, 85:587–600.

[52] Y. Urano, K. Kikuchi, H. Kojima, T. Nagano, J. Am, Highly Sensitive Fluorescence Probes for Nitric Oxide Based on Boron Dipyrromethene Chromophore—Rational Design of Potentially Useful Bioimaging Fluorescence Probe, Chem. Soc. 2004, 126:3357–3367.

[53] Boens N, Leen V, Dehaen W. Fluorescent indicators based on BODIPY. Chem Soc Rev 2012, 41:1130- 17241

[54] Hayashi YT, Stasevich TJ, Kurumizaka H, Nozaki N, Kimura H. Evaluation of chemical fluorescent dyes as a protein conjugation partner for live cell imaging. PLoS One Sep 2014; 3:106271.

Scheme Caption

Scheme 1. Chemical structure and synthetic pathway of BODIPY-indole compound (**3**)

Scheme 2. Proposed binding mechanism of 3 with Cu^{2+}

Table Caption

Table 1. Crystal data and refinement parameters for **3**.

Figure Captions

Fig. 1. The asymmetric unit of compound 3. Displacement ellipsoids are drawn at the 30% probability level. H-atoms are shown as small spheres of arbitrary radii.

Fig. 2. UV–Vis absorption change profiles of compound **3** (5.0 μM) in CH_3CN with various metal ions (5.0 μM).

Fig. 3. UV–Vis absorption spectrum of **3** (5.0 μM) with gradual addition of Cu^{2+} in CH_3CN solution.

Fig. 4. Fluorescence responses of **3** (5.0 μM) in CH_3CN solution upon the addition of 1 equivalent of various metal ions (Excitation wavelength= 570 nm).

Fig. 5. Metal ions selectivity of molecule 3 (5.0 μM) in CH3CN solution. The red bars represent the fluorescent intensity of only 3 and the blue bars represent the fluorescent intensity of 3 and various ions (Excitation wavelength= 570 nm).

Fig. 6. Fluorescence titration of compound **3** (5.0 μM) with various concentration of Cu^{2+} in CH_3CN solution (Excitation wavelength= 570 nm). Inset: Fluorescence decay profile of compound **3** in the presence and absence of Cu^{2+} using laser excitation source of 674 nm

Fig. 7. Fluorescence intensity of **3** versus Cu^{2+} ions. [compound **3**] = 5 μM

Fig. 8. The Job's plot for compound 3 and Cu^{2+} (Excitation wavelength= 570 nm).

Fig. 9. Plot of $1/F\text{-}F_0$ against **3**/[Cu^{2+}] for compound **3** in CH_3CN solution.

Fig. 10. Solution colour of molecule **3** exposed to various types of cations under sunlight (top) and UV light (bottom).

Fig. 11. The photo stability of **3** and **3**-Cu^{2+}. The change of fluorescence intensity with irradiation time for molecule **3** and compound **3**-Cu^{2+}.

Fig. 12. Fluorescent image of 3 in mammalian cells**.** HuH7 cells were treated with 0.1 μM of compound **3** and incubated for 15 minutes. **A.** Bright field image **B.** TritC filtered image.

Fig. 13. Fluorescent image of molecule **3** in bacterial cells**.** *Bacillus thuringiensis* cells were treated with 0.1 μM of **3** and incubated for 15 minutes. **A.** Bright field image. **B.** TritC filtered image.

Fig. 14. Flow cytometry analysis of fluorescent **3** stained mammalian cells. HuH7 cells were stained with 0.1 μM and 5 μM of compound **3**. Overlay histogram of cells, unstained, stained with both 0.1 μM of and 5 μM of **3**. Cell excited with red laser and data obtained from FL4: 675/25 nm filter.

Fig. 15. Cytotoxic effects of **3** on bacterial and mammalian cells. **A.** Bacterial cells were treated with 100 μM of compound **3** and incubated for 24 hours. Viable cells count compared with DMSO treated control cells and calculated as cfu/ml. **B.** MTS assay results of HuH7 cells which were treated with 0.1, 0.5, 1, 5, 100 μM of compound **3** and incubated for 24 hours. Percentage of viable cells compared with DMSO treated control cells (set at 100%). Bars represent the corresponding standard deviations (n=3).

Naked-Eye Fluorescent Sensor for Cu (II) Based on Indole Conjugate BODIPY Dye

Sureyya O. Tümay[a] , Elif Okutan[a], Ibrahim F. Sengul[a], Emrah Özcan[a], Hakan Kandemir[b], Tuğrul Doruk[c], Metin Çetin[c], Bünyemin Çoşut[a*]

Contribution from:

[a] Department of Chemistry, Faculty of Science, Gebze Technical University, Gebze, Kocaeli, Turkey

[b] Department of Chemistry, Faculty of Art and Science, Namık Kemal University, Tekirdag, Turkey

[c] Department of Molecular Biology and Genetics, Faculty of Science, Gebze Technical University, Gebze, Kocaeli, Turkey

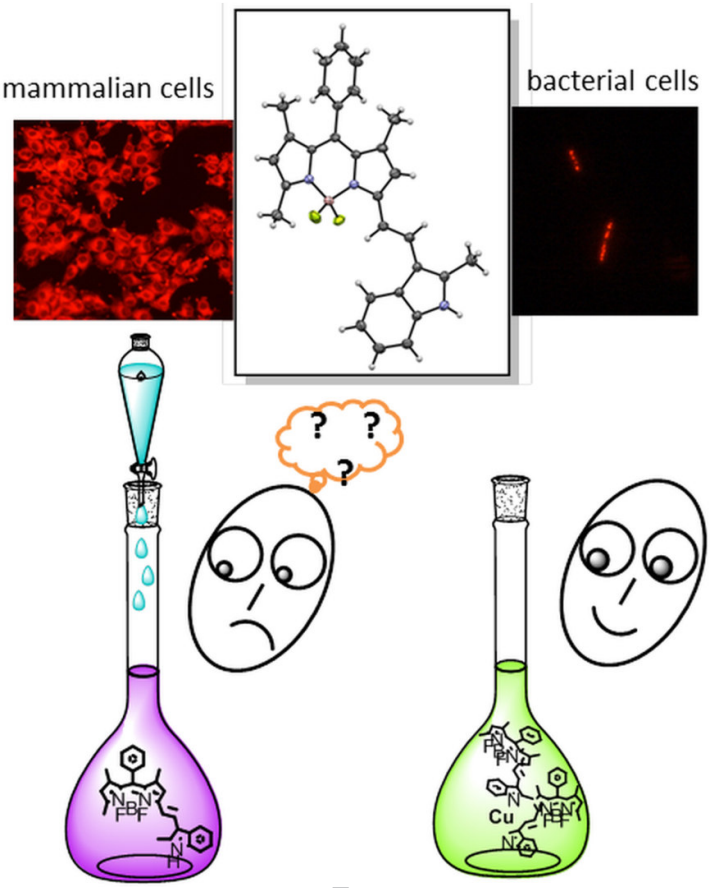

Naked-Eye Fluorescent Sensor for Cu (II) Based on Indole Conjugate BODIPY Dye

Sureyya O. Tümay[a] , Elif Okutan[a], Ibrahim F. Sengul[a], Emrah Özcan[a], Hakan Kandemir[b], Tuğrul Doruk[c], Metin Çetin[c], Bünyemin Çoşut[a*]

Contribution from:

[a] Department of Chemistry, Faculty of Science, Gebze Technical University, Gebze, Kocaeli, Turkey

[b] Department of Chemistry, Faculty of Art and Science, Namık Kemal University, Tekirdag, Turkey

[c] Department of Molecular Biology and Genetics, Faculty of Science, Gebze Technical University, Gebze, Kocaeli, Turkey

A novel indole mono-styryl BODIPY was synthesised and characterized for the colorimetric recognition of Cu^{2+}. It was also revealed from this study 3 can passively diffuse through cell membrane and stain both bacterial and mammalian cells even in very low concentrations. BODIPY-indole 3 retains inside the cells in cytometry and can be further modified for other applications.